Supplementary Information

Interactions between Glutamate, Dopamine, and the Neuronal Signature of Response Inhibition in the Human Striatum

Supplementary Results: Neuronal signature of stop signal task

A one-sample *t*-test was calculated using differential t-contrast images of successful stop trials versus go trials from the single subject level. Whole brain effects were corrected for multiple comparisons using a whole brain FWE-correction with an error probability of $p < 0.05$. This analysis revealed a well established network, which includes frontal areas (bilateral middle and inferior frontal gyri, bilateral insular cortex, medial frontal areas), parietal areas (bilateral inferior parietal lobule, left angular gyrus, and right superior parietal lobule), occipital areas (left middle occipital gyrus, right calcarine gyrus, right lingual gyrus, and right superior occipital gyrus), left cerebellum and bilateral nucleus caudate (see Supplementary Table S1 and Supplementary Fig. S3). A similar fronto-parietal-stiatal network was also found in a recent meta-analysis by Swick et al. [2011] including 21 stop signal articles. The additional activation differences in the occipital areas are probably related to the visual stimulation: The current study employed a visual stop cue, whereas other studies often use auditory stop cues, e.g. Ghahremani et al. [2012].

Supplementary Results: Mediator Analysis

As an additional control analysis we calculated a moderator analysis [Hayes, 2013]. Please note that mathematically a multiple linear regression is equal to moderator analysis. We first calculated the simple linear regression without moderator (glutamate concentration): The linear regression with dopamine synthesis capacity as predictor for the neural signature of response inhibition revealed a significant result (ANOVA: $F(28)=7.2$, $p=0.012$, $R^2=0.211$; coefficient: $\beta(\text{dopamine})=0.459, p=0.012$). When adding glutamate and the interaction between dopamine and glutamate to the regression (equivalent to moderator analysis), the regression model remained significant (ANOVA: $F(28)=8.8$, $p<0.001$) and explained an increase in variance ($R^2=0.514$; regression coefficients: $\beta(\text{dopamine})=0.219$, $p=0.173$, $\beta(\text{glutamate})=0.584$, $p=0.001$, $\beta(\text{dopamine*glutamate})=-0.105$, $p=0.467$). The unstandardized simple slope for participants 1 SD below the mean of glutamate concentration was 0.36, the unstandardized simple slope for participants with a mean level of glutamate concentration was 0.24, and the unstandardized simple slope for participants 1 SD above the mean of glutamate concentration was 0.11.

References

Ghahremani DG, Lee B, Robertson CL, Tabibnia G, Morgan AT, De Shetler N, Brown AK, Monterosso JR, Aron AR, Mandelkern MA, Poldrack RA, London ED (2012): Striatal dopamine D2/D3 receptors mediate response inhibition and related activity in frontostriatal neural circuitry in humans. J Neurosci Off J Soc Neurosci 32:7316–7324.

Hayes AF (2013): Introduction to Mediation, Moderation, and Conditional Process Analysis: A Regression-Based Approach 1st ed. New York u.a.: Guilford Pubn.

Swick D, Ashley V, Turken U (2011): Are the neural correlates of stopping and not going identical? Quantitative meta-analysis of two response inhibition tasks. NeuroImage 56:1655–1665.

Supplementary Table S1. fMRI whole brain results of stop signal task. Effect of successful stop against go trials for one sample *t*-test is reported using a whole brain FWE-correction with an error probability of p <0.05.

Brain structure	Hem	Cluster size (vox)	T (peak)	p_{FWE} (peak)	MNI coord. (mm) of local maximum x	y	z
Middle Occipital Gyrus	L	831	14.74	<0.001	-30	-94	-5
Middle Occipital Gyrus	L		13.04	<0.001	-15	-100	-2
Middle Occipital Gyrus	L		12.44	<0.001	-27	-94	7
Lingual Gyrus	R	738	14.77	<0.001	27	-88	-5
Superior Occipital Gyrus	R		13.55	<0.001	24	-100	7
Calcarine Gyrus	R		13.05	<0.001	18	-100	-2
Middle Temporal Gyrus	R	655	9.45	<0.001	66	-40	-2
Inferior Parietal Lobule	R		8.56	<0.001	48	-58	49
Superior Parietal Lobule	R		8.37	<0.001	36	-58	55
Superior Parietal Lobule	R	4	6.08	0.015	18	-67	55
Inferior Temporal Gyrus	R	1	5.80	0.036	45	8	-41
Inferior Temporal Gyrus	R	1	5.74	0.043	42	5	-44
Angular Gyrus	L	111	7.90	<0.001	-51	-52	34
Inferior Parietal Lobule	L		7.39	<0.001	-48	-49	58
Inferior Parietal Lobule	L		7.12	0.001	-60	-46	37
Inferior Parietal Lobule	L	15	6.85	0.001	-36	-46	40
Middle Temporal Gyrus	L	6	6.15	0.012	-54	-55	10
Middle Temporal Gyrus	L	6	6.48	0.004	-63	-61	7
Inferior Parietal Lobule	L	1	5.70	0.049	-36	-58	46
Middle Temporal Gyrus	L	1	5.86	0.030	-54	-34	-11
Middle Frontal Gyrus	R	412	8.78	<0.001	48	14	49
Middle Frontal Gyrus	R		8.16	<0.001	42	14	55
Middle Frontal Gyrus	R		7.86	<0.001	42	5	58
Middle Frontal Gyrus	R	4	6.14	0.012	27	59	25
Middle Frontal Gyrus	L	106	7.46	<0.001	-39	47	4
Middle Frontal Gyrus	L		7.01	0.001	-39	59	4
Inferior Frontal Gyrus (p. Orbitalis)	L		6.77	0.002	-39	50	-11
Inferior Frontal Gyrus (p. Orbitalis)	L	3	6.28	0.008	-54	32	-8
Middle Frontal Gyrus	L	88	7.92	<0.001	-51	26	34
Precentral Gyrus	L		7.21	<0.001	-54	14	40
Middle Frontal Gyrus	L		6.21	0.010	-45	35	31
Precentral Gyrus	L	2	6.02	0.018	-33	2	37
Precentral Gyrus	L	1	6.04	0.017	-42	-1	61
Middle Frontal Gyrus	L	1	5.58	0.020	-48	5	55
Insula Lobe	R	360	9.64	<0.001	36	23	-5
Inferior Frontal Gyrus (p. Orbitalis)	R		8.83	<0.001	45	23	-8
Inferior Frontal Gyrus (p. Triangularis)	R		7.86	<0.001	51	47	-2
Insula Lobe	L	49	8.82	<0.001	-33	20	1
Superior Medial Gyrus	L	21	6.93	0.001	-3	32	43
Superior Medial Gyrus	R		5.34	0.007	3	26	49

Supplementary Motor Area (SMA)	L	2	6.03	0.017	-6	17	49
Superior Medial Gyrus	R	2	5.78	0.038	9	29	40
Caudate Nucleus	L	11	7.15	0.001	-9	5	7
Caudate Nucleus	R	2	6.10	0.014	9	5	4
Caudate Nucleus	R	1	5.82	0.034	12	8	7
Cerebellum	L	25	6.65	0.003	-21	-73	-29
Cerebellum	L		6.35	0.006	-9	-79	-29

Please note that different brain regions are grouped together even when there were several distinct clusters. Different clusters are indexed by different cluster size numbers. When no number is present the local maximum of this location is part of the previous named cluster.

Supplementary Table S2. Effect of Age and Gender on inhibition performance (SSRT) and multimodal imaging modalities. SSRT = stop signal reaction time.

	Age (Correlation)	Gender (T-Test)
SSRT	$r(38) = 0.367$, $p = 0.023$	$T(36) = 0.074$, $p = 0.94$
Dopamine Synthesis Capacity	$r(38) = -0.172$, $p = 0.302$	$T(36) = 0.517$, $p = 0.609$
Glutamate Concentration	$r(29) = -0.273$, $p = 0.152$	$T(27) = -0.8$, $p = 0.43$
Inhibition-related neuronal activity	$r(38) = -0.257$, $p = 0.12$	$T(36) = 0.95$, $p = 0.351$

Figure Legends

Supplementary Figure S1. MRS voxel placement in the striatum. Illustration of the voxel placement in the left striatum of a representative participant. The MRS voxel was individually placed before each MRS measurement. MRS = magnetic resonance spectroscopy.

Supplementary Figure S2. fMRI results of stop signal task. Effect of successful stop against go trials during the stop signal task is illustrated for the one sample *t*-test (whole brain FWE-correction with an error probability of $p < 0.05$, n = 38). The upper two panels show the left (left panel) and right (right panel) hemisphere, whereas the bottom left panels shows the top view on the brain. On the bottom right panel is a coronal slice (y=7) depicted showing the activation difference in the bilateral nucleus caudate.

Supplementary Figure S3. Mean parameter estimates of the significant effect in the left caudate nucleus for successful stop against go trials (cluster size: 11 voxels, see also Figure S2, bottom right panel)

Supplementary Figure S4. Relationship between inhibition-related neuronal activity in the nucleus caudate (mean parameter estimates of the significant effect in the caudate nucleus for successful stop against go trials) with inhibition performance (SSRT). SSRT = stop signal reaction time, a.u. = arbitrary units.

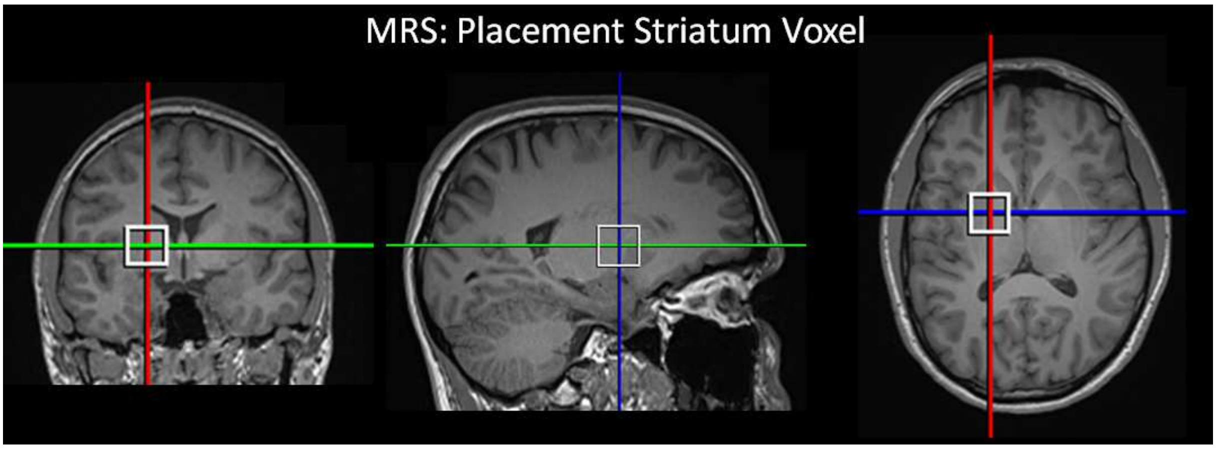

Supplementary Figure S1

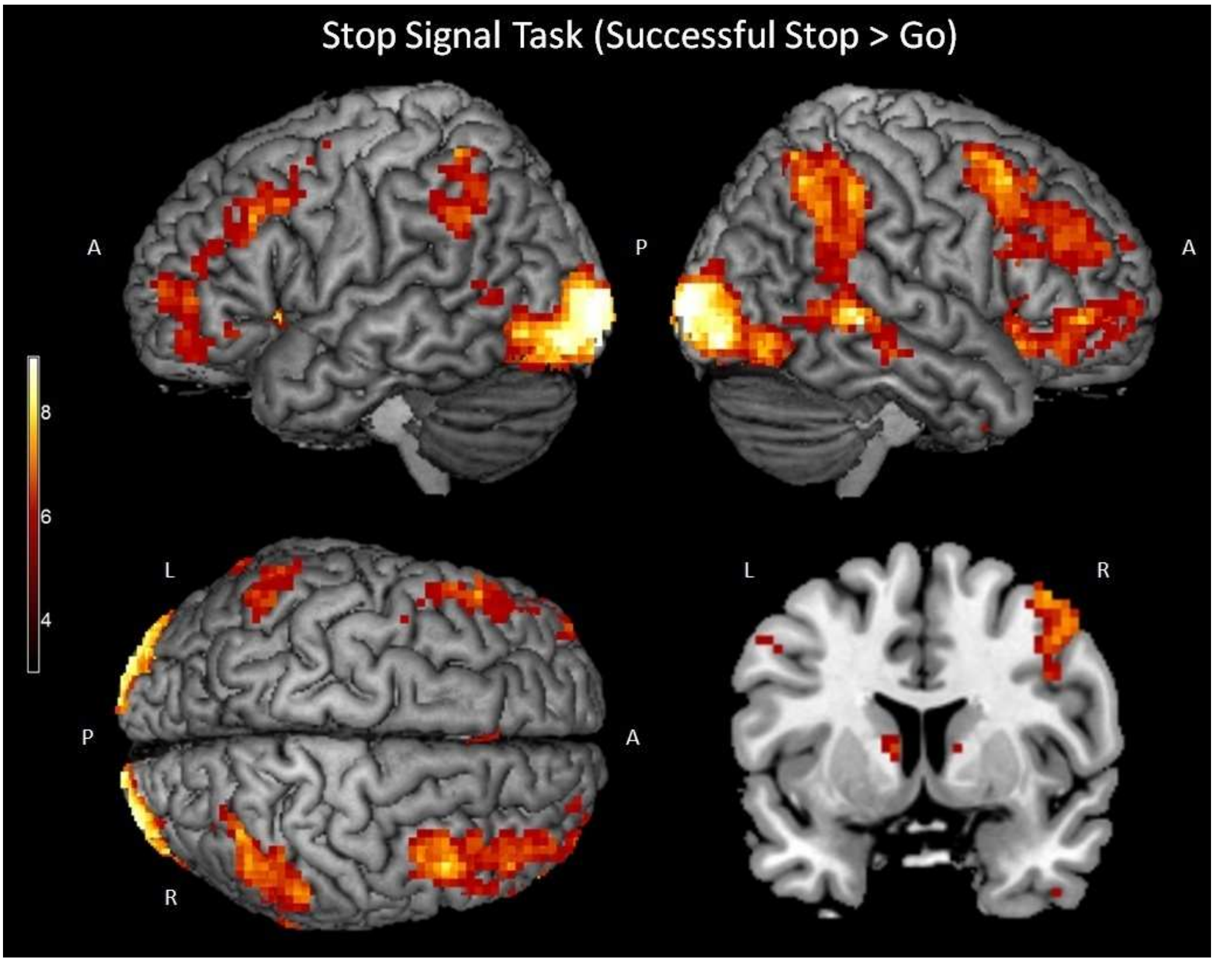

Supplementary Figure S2

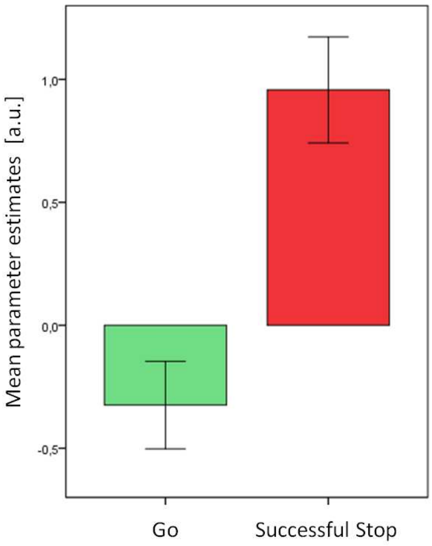

Supplementary Figure S3

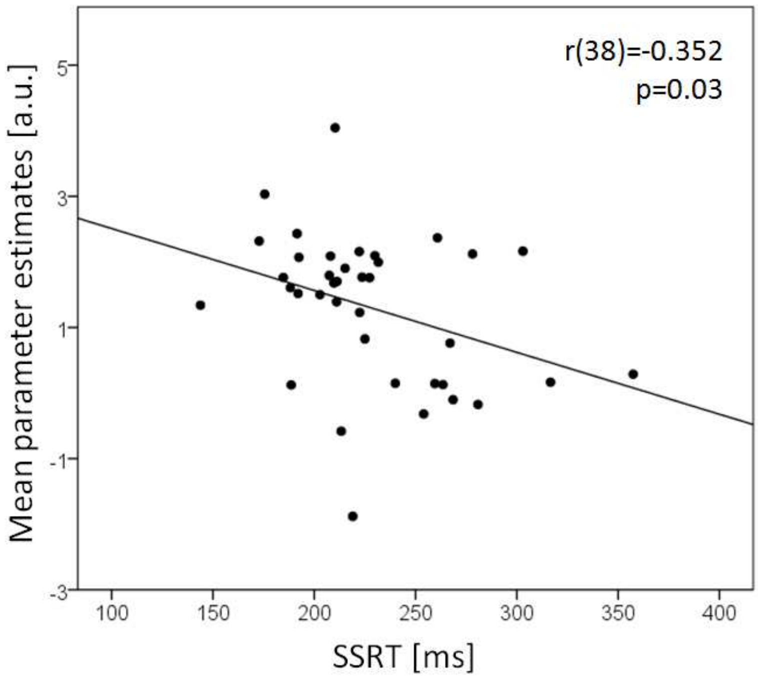

Supplementary Figure S4